Deep eutectic solvent-based manganese dioxide nanosheets composites for determination of DNA by a colorimetric method

Jia Xu[1*], Yuan Yang[1], Juan Du[1], Hui Lu[1], Wenqi Gao[1], Hongjian Gong[1] and HanXiao[1*]

Abstract

Background Nucleic acid is the carrier of genetic information and the keymolecule in life science. It is important to establish a simple and feasible method for nucleic acid quantification in complex biological samples.

Methods Four kinds of hydrogen bond acceptors (choline chloride (ChCl), L-carnitine, tetrabutylammonium chloride (TBAC) and cetyltrimethylammonium bromide (CTAB)) were used to synthesize deep eutectic solvents (DESs) with hexafluoroisopropanol (HFIP). DESs based manganese dioxide (MnO_2) nanosheets composites was synthesized and characterized. DNA concentration was determined by a UVVis spectrometer. The mechanism of DNA-DES/MnO_2 colorimetric system was further discussed.

Results The composite composed of DES/MnO_2 exhibited excellent oxidase-like activity and could oxidize 3,3′,5,5′-tetramethylbenzidine (TMB) to produce a clear blue change with an absorbance maximum at 652 nm. When DNA is introduced, the DNA can interact with the DES by hydrogen bonding and electrostatic interactions, thereby inhibiting the color reaction of DES/MnO_2 with TMB. After condition optimization, ChCl/HFIP DES in 1:3 molar ratio was used for the colorimetric method of DNA determination. The linear range of DNA was 10–130 μg/mL and exhibited good selectivity.

Conclusion A colorimetric method based on DES/MnO_2 was developed to quantify the DNA concentration. The proposed method can be successfully used to quantify DNA in bovine serum samples.

Keywords Hexafluoroisopropanol, Deep eutectic solvents, Manganese dioxide nanosheets, Nucleic acid, Colorimetry

*Correspondence:
Jia Xu
xujia0113@hust.edu.cn
HanXiao
tjxiaohan@hust.edu.cn
[1]Institute of Maternal and Child Health, Wuhan Children's Hospital
(Wuhan Maternal and Child Healthcare Hospital), Tongji Medical College,
Huazhong University of Science & Technology, 430016 Wuhan, China

Introduction

Deep eutectic solvents (DESs), an emerging class of environmentally friendly solvents are formed by hydrogen bond acceptors (HBAs) and hydrogen bond donors (HBDs) in an appropriate ratio. The formation of strong hydrogen bonds leads to a melting point lower than that of each individual component [1]. DESs possess numerous excellent properties including low volatility, ease of storage, stable physical and chemical properties, and good biocompatibility [2, 3]. In addition, the physical or chemical properties of DESs can be tuned by selecting HBAs and HBDs species [4, 5]. Owing to their excellent biocompatibility, DESs have been widely applied in the partitioning of biomass, such as proteins and, nucleotides, and for improving the efficiency of enzymatic reactions [6–11].

Nucleic acid, the carrier of genetic information, is a crucial molecule in life sciences. High-purity nucleic acids are the foundation of studies in clinical trials, genomics, food safety and other fields [12, 13]. However, real samples of nucleic acid usually contain impurities such as metal ions and proteins, which interfere with the reliability of the experimental analysis. Consequently, establishing a convenient and simple method for the accurate quantification of nucleic acids in complex biological samples is of great significance. DESs have been used as green substitutes for traditional organic solvents for nucleic acid extraction from aqueous solutions [8, 9, 11, 14]. In addition, Mondal et al. reported the solubility of DNA in DESs and confirmed the chemical and structural stability of DNA after six months of storage in DESs comprising glycerol and ethylene glycol [15]. Sharma et al. reported that hydrogen bonding is the major driving force that promotes the dissolution of DNA in DESs [16]. A recent and promising improvement in DES-based DNA purification approaches is the use of a combination of nanomaterials [2, 17–19].

Manganese dioxide (MnO_2) is a functional transition metal oxide and its nanosheets have unique properties, such as a high specific surface area and oxidase-mimicking activity [20, 21]. It has been applied in sensing technology [22, 23], cell imaging [24], magnetic resonance imaging [25], and biomedical analysis [26–28]. 3,3',5,5'-Tetramethylbenzidine (TMB) is a commonly used chromogenic substrate that can change from colorless to blue in the presence of MnO_2 nanosheets with oxidase-like activity [29]. A colorimetric method based on MnO_2 nanosheets/TMB has been reported for the detection and quantification of target compounds and biomacromolecules, including glucose, pesticides, metal ions, antibacterial agents, and nucleic acid [14, 20–22, 29, 30].

Hexafluoroisopropanol (HFIP) is a perfluorinated alcohol with a high density and strong hydrophobicity [31]. HFIP has proven to be an excellent HBD for preparation of high-density HFIP-based DESs with various HBAs [4, 32]. At present, HFIP-based DESs have been successfully employed in the purification of pesticides, anthraquinones, and dyes [4, 31, 33], but they are also used as environmental reaction media [34]. In this study, HFIP-based DESs combined MnO_2 nanosheets were synthesized and employed for the quantification of DNA for the first time. Choline chloride (ChCl) was selected as the HBA to synthesize the DES with HFIP. The DNA quantification procedure was based on the colorimetric reaction between DES/MnO_2 and TMB. We demonstrated that this method could accurately quantify DNA from bovine serum samples.

Materials and Methods

Materials

Cetyltrimethylammonium bromide (CTAB), sodium acetate (NaAc), anhydrous acetic acid, $KMnO_4$, NaOH, $(NH_4)_2SO_4$, K_2HPO_4, KH_2PO_4, Na_2CO_3, Na_2HPO_4 and Na_2SO_4 were purchased from Sinopharm Chemical Reagent Co., Ltd. (Shanghai, China). Salmon sperm DNA sodium salt, morpholine ethanesulfonic acid (MES), HFIP, ChCl, L-carnitine, tetrabutylammonium chloride (TBAC), and TMB were purchased from Macklin (Shanghai, China). Bovine serum was purchased from Haoyang Biological Manufacture Co., Ltd. (Tianjin, China). All other reagents were of analytical grade and were commercially available. Deionized (DI) water (18.25 MΩ) was used in all the experiments.

Instrumentation

The surface modification of the obtained DES and DES/MnO_2 was investigated using a Nicolet 470 fourier transform infraed (FT-IR) spectrometer (Thermo Fisher Scientific, USA) in a KBr pellet at room temperature. Nuclear magnetic resonance (^{1} H NMR) spectra were obtained using an Avance III 400 MHz spectrometer (Bruker, Germany) and the morphology of the MnO_2 nanosheets was observed using a JEM-2100 transmission electron microscope (TEM) (JEOL, Japan). Thermal gravimetric analysis (TGA) was performed using TG 209F1 (NETZSCH, Germany). A PHI5000 VersaProbe (PHI, Japan) was used for X-ray photoelectron spectroscopy (XPS) analysis. The zeta potential and dynamic light scattering (DLS) were analyzed using a Zeta sizer Nano ZS90 (Malvern, England). Agitation and extraction were performed using an UXI orbital shaker (Huxi, China). The concentration of the DNA solution was determined using a UV-1600PC ultraviolet-visible (UV-Vis) spectrophotometer (XIPU, China). The obtained MnO_2 nanosheets were dried using an XMTD-8222 vacuum dryer (Jinghong, China). The obtained DES-MnO_2 was dried in a ZX-LGJ-1 A freeze dryer (Zhixin, China).

Preparation of DES

Four types of DESs (ChCl/HFIP, L-carnitine/HFIP, TBAC/HFIP, and CTAB/HFIP) were synthesized by stirring a designed amount of HBAs and HFIP in a 150 mL thick-walled pressure-resistant flask at an appropriated temperature until a homogeneous transparent liquid was formed. After optimization, a DES composed of ChCl/HFIP at a 1:3 molar ratio was prepared.

Preparation of MnO$_2$ nanosheets

MnO$_2$ nanosheets were synthesized according to a previous reported method [35, 36]. 20 mg KMnO$_4$ was accurately weighed and transferred to a 50 mL conical flask, dissolved in 18 mL of DI water, and stirred for 1 h at room temperature. Subsequently, 60 mg of CTAB was added to the flask and stirred continuously until a stable emulsion was formed. Next, 2 mL of 0.1 mol/L MES was poured into the mixture and reacted for 6 h. Finally, the MnO$_2$ nanosheets were washed three times with DI water. After centrifuging at 12,000 rpm for 5 min, the MnO$_2$ nanosheets were dried at 60 °C under vacuum.

Preparation of DES/MnO$_2$

DES/MnO$_2$ was prepared using a previously reported method [14] with some modifications. Briefly, 20 mg of MnO$_2$ nanosheets were dispersed in 2 mL of methanol and 0.5 mL of synthesized ChCl/HFIP DES and the mixture was ultrasonicated for 2 h at room temperature. The resulting solution was centrifugated at 5000 rpm for 10 min and washed three times with methanol. Finally, the DES/MnO$_2$ solid was collected by vacuum freeze-drying.

Colorimetric reaction of DES/MnO$_2$ and TMB

50 µL of TMB (2 mg/mL) was dissolved in 1800 µL NaAc (pH 4.0). Subsequently, 150 µL DES/MnO$_2$ of different concentrations were added to this above mixed solution and shaken on an incubator shaker for 30 min at room temperature. Finally, the resulting solution was measured at 652 nm by UV-Vis spectrometer.

Colorimetric determination of DNA concentration

Next, 150 µL of DES/MnO$_2$ (0.1 mg/mL) was added to 1750 µL NaAc (pH 4.0) aqueous solution. Therefore, 50 µL of DNA solutions with different concentrations was added to the mixed solution. After the addition of 50 µL TMB (2 mg/mL), the mixture was shaken for 30 min at room temperature. Finally, the absorbance of the resulting solution was measured at 652 nm using a UV-Vis spectrometer.

An aqueous solution of 150 µL DES/MnO$_2$ (0.1 mg/mL), 50 µL TMB (2 mg/mL), and 1850 µL NaAc (pH 4.0) was prepared to conduct selectivity experiments. Various non-specific proteins, carbohydrates, and salts were selected to replace DNA and were added to the prepared aqueous solution for the DNA selectivity test. The mixture was then shaken for 30 min at room temperature. Finally, the absorbance of the resulting solution was measured at 652 nm using a UV-Vis spectrometer.

## Results and discussion

Preliminary studies

ChCl, L-carnitine, TBAC, and CTAB were selected as HBA, and HFIP was selected as the HBD. To determine the extraction potential of the proposed DESs for DNA extraction, six inorganic salts ((NH_4)$_2SO_4$, K_2HPO_4, KH_2PO_4, Na_2CO_3, Na_2HPO_4, and Na_2SO_4) were used as phase separation inducers. A system of 0.5 mL DES (ChCl/HFIP, L-carnitine/HFIP, TBAC/HFIP, and CTAB/HFIP) and 0.8 g inorganic salts ((NH_4)$_2SO_4$, K_2HPO_4, KH_2PO_4, Na_2CO_3, Na_2HPO_4, and Na_2SO_4) were prepared in 5 mL of aqueous solution. The molar ratio of HBAs to the HFIP was 1:2. DNA (10 µg/mL) was added to investigate the extraction performance of the two-phase system. After separating into two phases, the bottom phase was removed and detected at 260 nm using a UV detector. The extraction results are summarized in Table S1. It can be seen that the DES comprising ChCl and HFIP was suitable for DNA extraction.

Figure S1 shows the effect of the ChCl:HFIP molar ratio on DNA extraction. A system involving 0.5 mL DES with different molar ratios (1:1.5, 1:2, 1:3, and 1:4) and 0.8 g Na_2SO_4 was prepared in 5 mL of aqueous solution. It was clear that DNA extraction increased with the molar ratio varying from 1:1.5 to 1:3 and thereafter a declined at molar ratio of 1:4. In conclusion, a DES comprising ChCl and HFIP in a 1:3 molar ratio was suitable for DNA extraction.

Characterization of DES and DES/MnO$_2$

FT-IR spectra and ^{1}H NMR were used to characterize the synthesized DESs. As shown in Fig. S2 the stretching vibration peaks of O-H in pure HFIP and ChCl were observed at 3424 cm^{-1} and 3293 cm^{-1}, respectively, which shifted to a lower wavenumber of 3165 cm^{-1} in ChCl/HFIP. The shift of the –OH stretching vibration indicated the existence of hydrogen bonding between ChCl and HFIP. In addition, no new peaks were detected, demonstrating that no chemical reaction occurred during DES synthesis. As shown in Fig. S3, the ^{1}H NMR of ChCl/HFIP is as follows: δ 4.60 (s, 1 H), 4.01 (dd, 2 H), 3.52 (m, 2 H), 3.21 (d, 9 H). These results verified that the HFIP/ChCl DES was successfully synthesized.

The high-resolution TEM image of the prepared MnO$_2$ nanosheets (Fig. 1a) revealed the presence of large two-dimensional sheet-like structures, which provided a large surface area for the reaction with TMB, a chromogenic substrate. Figure 1b shows the FT-IR characterization

Xu *et al. BMC Chemistry*   (2023) 17:15

Page 4 of 9
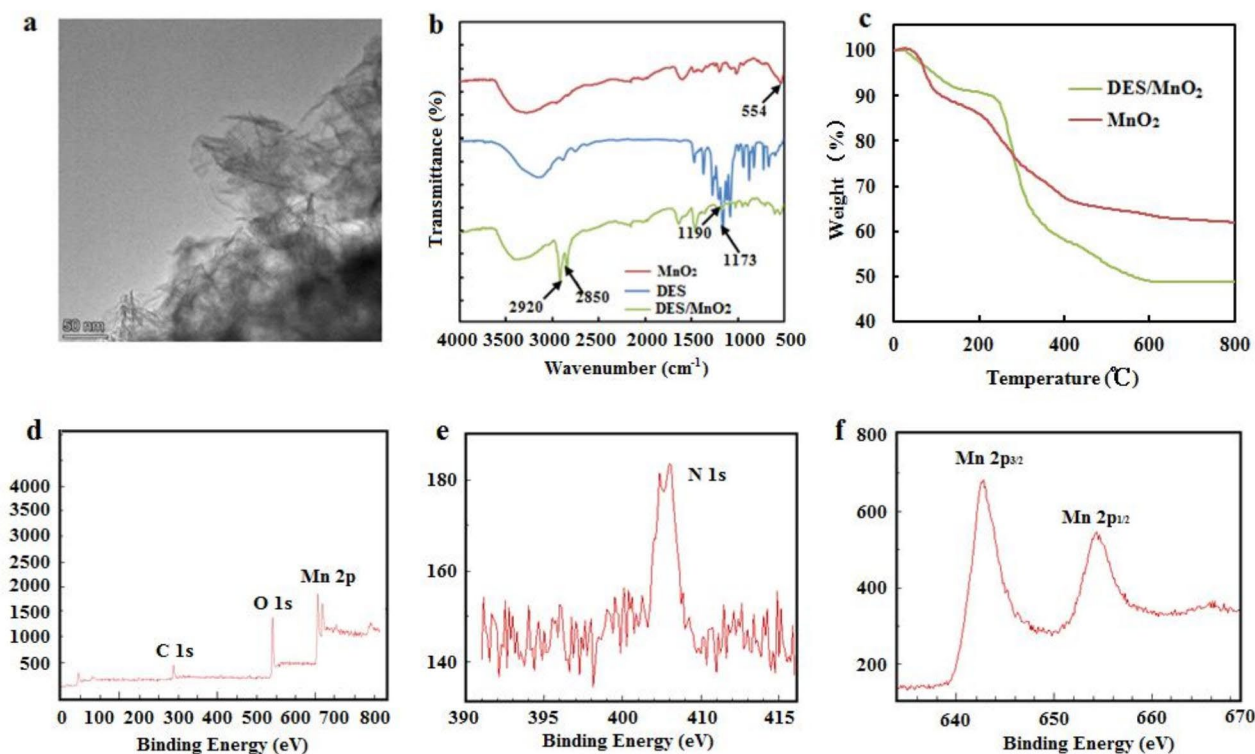
Fig. 1 (**a**) The TEM image of MnO_2 nanosheets; (**b**) FT-IR spectra of MnO_2 nanosheets, ChCl/HFIP DES and DES/MnO_2; (**c**) TGA of the MnO_2 nanosheets and DES/MnO_2; (**d**) The XPS full scan spectrum of DES/MnO_2; (**e**) The XPS spectrum of N 1s; (**f**) The XPS spectrum of Mn 2p

spectrum of the MnO_2 nanosheets, DES, and DES/MnO_2, where the MnO_2 nanosheets exhibited a distinct band at 554 cm^{-1}, which was attributed to Mn-O and Mn-O-Mn. The DES/MnO_2 spectrum revealed the presence of some characteristic peaks of DES, such as the absorption peaks at 2850 cm^{-1} and 2920 cm^{-1}, attributed to C-H, and the absorption peaks at 1173 cm^{-1} and 1190 cm^{-1} attributed to C-O. These results indicate the successful modification of the MnO_2 nanosheets by DES. TGA of the MnO_2 nanosheets and DES/MnO_2 (Fig. 1c) was performed to determine the mass percentages of the DES in the composites. The decomposition of the DES occurred at 225 °C with a mass loss of approximately 14%, indicating that the DES successfully modified the surface of the nanosheets at a grafting rate of approximately 14%. Figure 1d shows the high-resolution XPS profile of the DES/MnO_2. The N 1s spectrum (Fig. 1e) confirmed the presence of DES. Moreover, as shown in Fig. 1f, the two characteristic peaks with binding energies of 654.16 eV and 642.68 eV were attributed to the Mn $2p_{1/2}$ and Mn $2p_{3/2}$ of MnO_2, respectively. The XPS spectra also indicated the successful synthesis of DES/MnO_2.

DLS and zeta potential measurements were used to investigate the mechanism underlying the detection of DNA by DES/MnO_2. The zeta potential of the pure DNA, MnO_2 nanosheets, DES/MnO_2 and DNA-DES/MnO_2 were recorded. As shown in Fig. 2a, the zeta potential of the MnO_2 nanosheet was -23.77 mV. After combining with DES, the zeta potential of DES/MnO_2 was approximately -19.57 mV, which is slightly higher than that of the pure MnO_2 nanosheets. It was proven that the HFIP/ChCl DES was positively charged. Thus, the negatively charged DNA can bind to the DES through electrostatic interactions and thereafter adsorb onto the surface of DES/MnO_2. In addition, HFIP contains a large number of hydroxyl groups and is selected as the HBD in the synthesis of DES, which can enhance the hydrogen bond interaction between DES/MnO_2 and DNA. Therefore, the surface zeta potential of DNA-DES/MnO_2 was -22.9 mV, which is slightly lower than that of DES/MnO_2. Figure 2b shows the DLS results. The particle size of the DES/MnO_2 was approximately 342 nm. After combining with DNA, the size of the new aggregates was 459 nm, indicating that DNA-DES/MnO_2 was formed.

Measurement of the DES/MnO_2 oxidase activity
TMB was selected as the substrate to investigate the oxidase activity because DES/MnO_2 possess an oxidase-like activity and can directly oxidize TMB into oxidized TMB (oxTMB). Figure 3a shows neither a significant absorption peak (red) for DES/MnO_2 nor a significant absorption peak for TMB from 400 to 800 nm (blue).
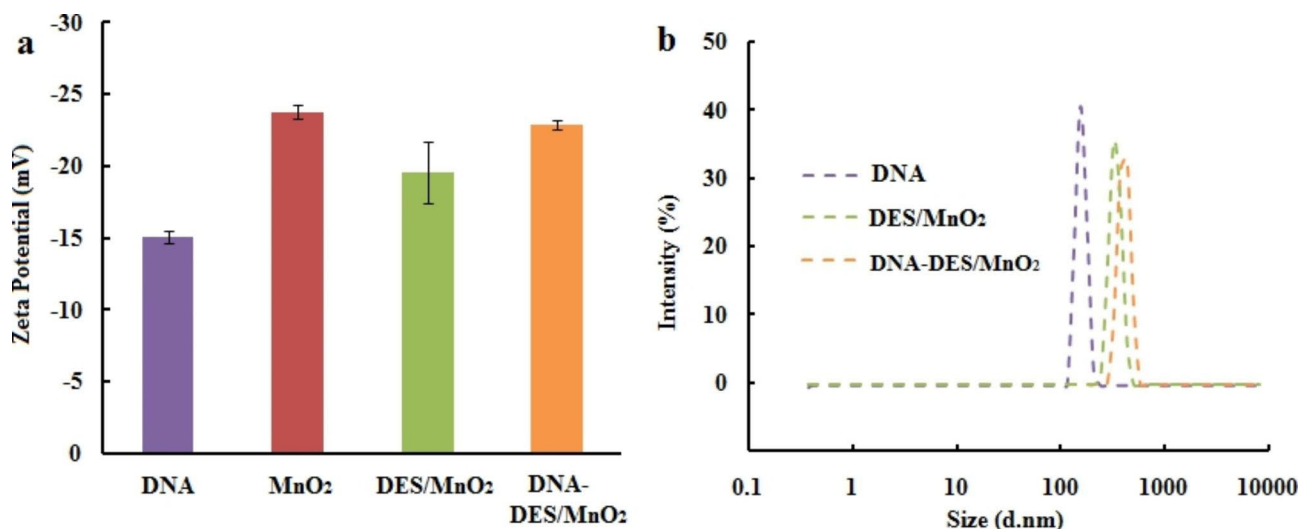
Fig. 2 Zeta potentials of DNA, MnO_2, DES/MnO_2 and DNA-DES/MnO_2 (**a**), and sizes distribution of DNA, DES/MnO_2 and DNA-DES/MnO_2 (**b**)
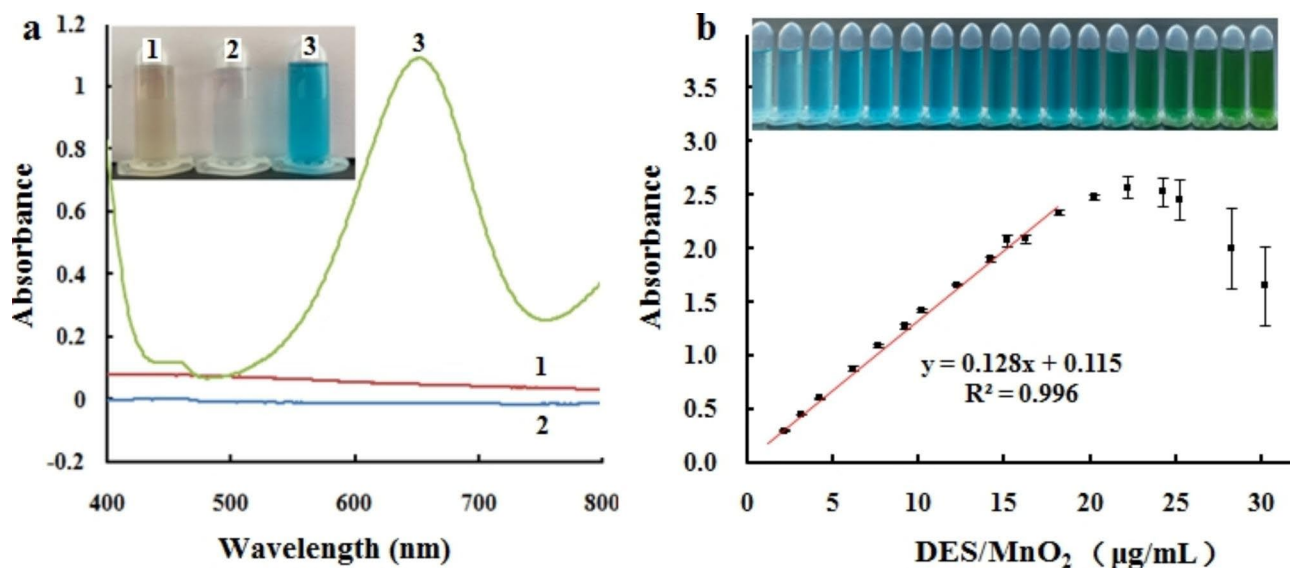
Fig. 3 UV absorption spectra of DES/MnO_2 (line 1), TMB (line 2), DES/MnO_2+TMB (line 3) and inset show the corresponding solution color (**a**); the absorbance intensity of DES/MnO_2-TMB system at different concentrations of DES/MnO_2 and inset shows the corresponding visual changes in color (**b**). All the error bars were calculated by three independent experiment (n = 3)

However, owing to the oxidase-like activity of the MnO_2 nanosheets, a deep blue color (characteristic absorption peak at 652 nm) was observed upon the binding of DES/MnO_2 with TMB owing to the oxidation of the colorless TMB.

To verify the catalytic activity of DES/MnO_2 further, different concentrations of DES/MnO_2 (0–30 µg/mL) were reacted with TMB. The absorbance gradually increased with increasing DES/MnO_2 concentration (Fig. 3b). However, the absorption intensity decreased when the concentration of DES/MnO_2 was higher than 22 µg/mL, because TMB or oxTMB may have been denatured. Figure 3b shows a series of color changes. Furthermore, the absorbance signal increased linearly with an

increase in the DES/MnO_2 concentration in the range of 0–18 µg/mL, and the linear regression had an equation of y = 0.128x + 0.115 (R^2 = 0.996).

The colorimetric reaction of the DES/MnO_2 composites with TMB under different pH conditions was thereafter evaluated (Fig. 4), and the strongest absorbance response was detected at pH 4.0, which was selected as the optimal pH.

Colorimetric determination of DNA concentration

To explore the utility of the DES/MnO_2-TMB system, a colorimetric quantitative analysis of DNA was performed under optimal conditions, and a standard curve was plotted. The difference in absorbance increased with
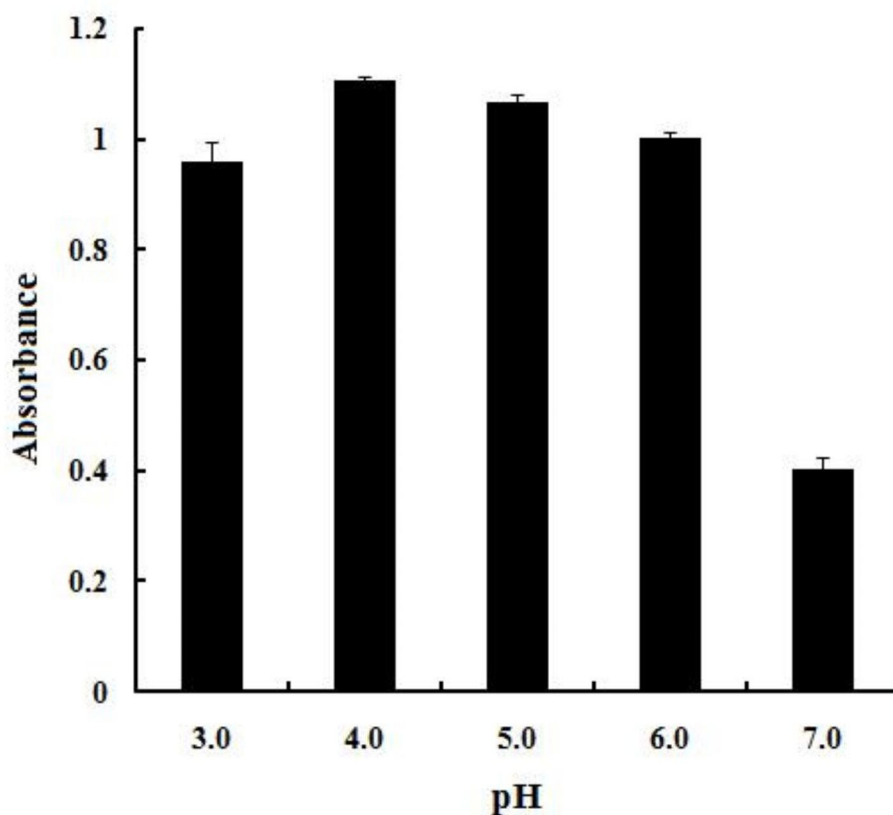
Fig. 4 Effect of the pH

an increase in DNA concentration until it eventually reached a plateau (the image depicts the gradual lightening of the solution color) (Fig. 5). Furthermore, the absorbance difference (ΔA), where ΔA denotes the difference in absorbance of the DES/MnO$_2$-TMB system before (A_0) and after (A) the addition of DNA, exhibited a good linear relationship with DNA concentration in the range of 10–130 μg/mL, and the linear equation was $y = 2.019x + 0.004$ ($R^2 = 0.996$). The adsorption of DNA onto the surface of DES/MnO$_2$ was mainly attributed to electrostatic interactions and hydrogen bonding between the phosphate group of DNA and the cationic part of the DES. With the addition of DNA adsorbed on the surface of DES/MnO$_2$, the colorimetric reaction of DES/MnO$_2$ with TMB was inhibited [21].

Specificity

To investigate the specificity of this method for DNA detection, the absorption spectral response of the DES/MnO$_2$-TMB system to various interfering substrates (non-specific proteins, carbohydrates, and salts) was studied (Fig. 6). The first column shows the absorption intensities of the DES/MnO$_2$-TMB system without the addition of DNA or other interfering substances. RNA had a greater effect on the absorption intensity,

whereas proteins such as bovine serum albumin (BSA), hemoglobin, and cytochrome C had a weaker effect. This is primarily because RNA has a structure similar to that of DNA, resulting in a similar inhibitory effect. Consequently, when testing samples containing both DNA and RNA, masking or pre-treatment steps are required.

Application to real samples

To evaluate the viability of our designed assay for practical applications, DES/MnO$_2$ was used to detect DNA in bovine serum. Different concentrations of DNA standard solution were spiked into the bovine serum samples to examine the recovery. The analytical results are summarized in Table 1. The recoveries were within the range of 102.73-107.08% for the three known concentrations of added DNA, and the relative standard deviation (RSD) was less than 3.63%. These results demonstrate the potential application of the proposed colorimetric method for the detection of DNA in real samples.

Conclusion

Herein, we report the synthesis of a DES/MnO$_2$ composite that efficiently catalyzes TMB. The composition and molar ratio of DESs were evaluated and DES composed of ChCl and HFIP with molar ratio of 1:3 was suitable for
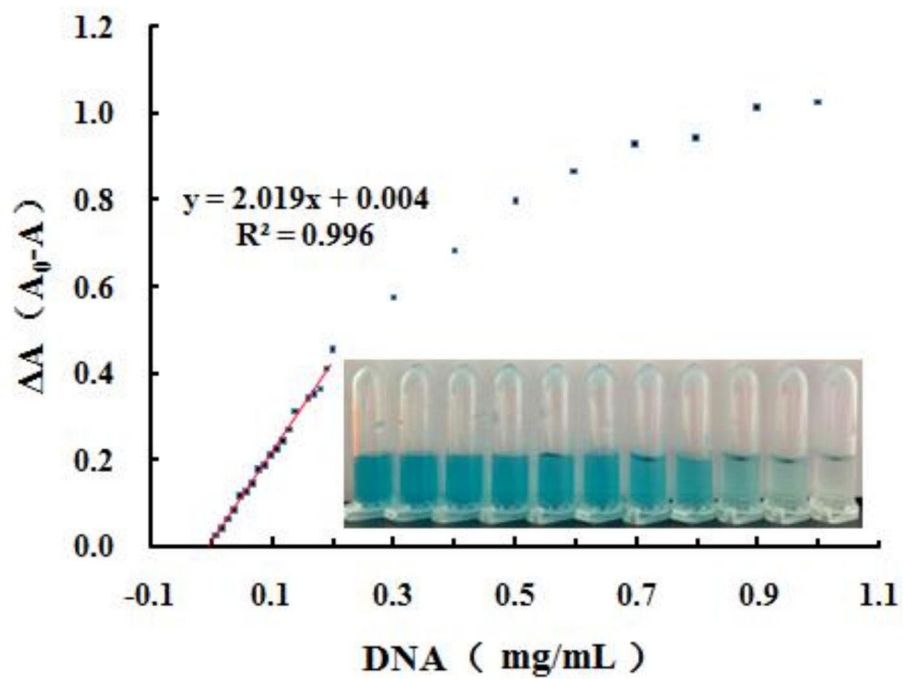
Fig. 5 Absorbance intensity of DES/MnO$_2$-TMB system at different concentrations of DNA and inset show the color change photographs
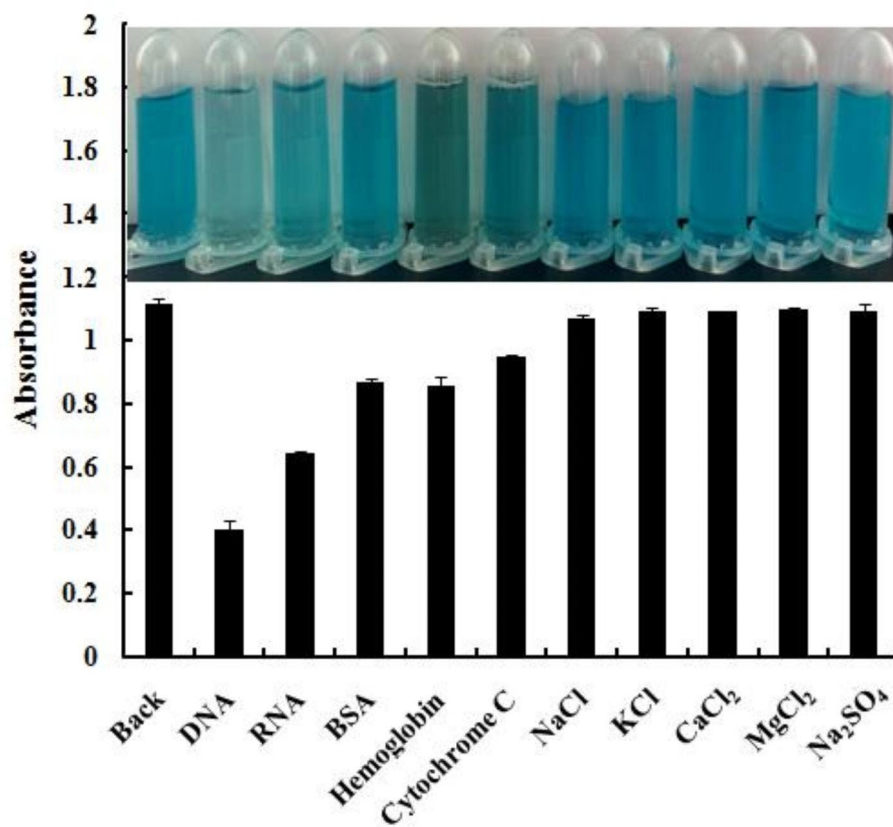
Fig. 6 Effect of interfering factors on DES/MnO$_2$ + TMB and inset show the color change photographs of DES/MnO$_2$-TMB system with different interfering factors

Xu *et al. BMC Chemistry*   (2023) 17:15

Page 8 of 9

Table 1 Determination of DNA in real sample of bovine serum ($n = 3$)

Added DNA (µg/mL)	Detected DNA (µg/mL)	Recovery (%)	RSD (%)
20.00	21.42	107.08	3.63
60.00	61.29	102.16	2.40
100.00	102.73	102.73	2.04

DNA extraction. The addition of DNA to the system significantly inhibited the colorimetric reaction and reduced the absorbance of DES/MnO_2-TMB owing to hydrogen bonding and electrostatic interactions between DNA and the DES. Consequently, a colorimetric method based on DES/MnO_2 was developed to quantify the DNA concentration. This method exhibited good linearity and specificity and could be used to determine DNA concentration in a simple and rapid manner. Consequently, it exhibits potential for application in DNA detection.

Abbreviations

DESs	Deep eutectic solvents
MnO_2	Manganese dioxide
TMB	3,3',5,5'-tetramethylbenzidine
HBAs	Hydrogen bond acceptors
HBDs	Hydrogen bond donors
DNA	Deoxyribonucleic acid
ChCl	Choline chloride
HFIP	Hexafluoroisopropanol
CTAB	Cetyltrimethylammonium bromide
NaAc	Sodium acetate
MES	Morpholine ethanesulfonic acid
UV-Vis	Ultraviolet-visible
NMR	Nuclear magnetic resonance
TEM	Transmission electron microscope
DLS	Dynamic light scattering
TGA	Thermal gravimetric analysis
XPS	X-ray photoelectron spectroscopy
oxTMB	Oxidized TMB
BSA	Bovine serum albumin

Supplementary Information

The online version contains supplementary material available at https://doi.org/10.1186/s13065-023-00922-5.

Table S1 The extraction efficiency of DESs with inorganic salts for the DNA extraction. Fig. S1 The effect of ChCl:HFIP molar ratio on DNA extraction. Fig. S2 FT-IR spectra of ChCl/HFIP DES. Fig. S3 ^{1}H NMR spectra of ChCl/HFIP DES. Table S2 The data for Fig. 6.

Acknowledgements
None declared.

Author contributions
JX: conceptualization, methodology, formal analysis, and writing-original draft. YY: methodology, formal analysis, and validation. JD: methodology, formal analysis, and validation. HL: methodology, data curation. WG: data curation. HG: data curation. HX: writing-review & editing, supervision, and project administration. All authors read and approved the final manuscript.

Data Availability
The datasets used and/or analyzed during the current study are available from the corresponding author on reasonable request.

Declarations

Ethics approval and consent to participate
Not applicable.

Consent for publication
Not applicable.

Competing Interest
The authors declare that they have no competing interests.

References

1. Ramezani AM, Ahmadi R, Yamini Y. Homogeneous liquid-liquid micro-extraction based on deep eutectic solvents. Trac-Trend Anal Chem. 2022;149:116566.
2. Peng F, Liu M, Wang X, Ding X. Synthesis of low-viscosity hydrophobic magnetic deep eutectic solvent: selective extraction of DNA. Anal Chim Acta. 2021;1181:338899.
3. Shakirova F, Shishov A, Bulatov A. Hydrolysis of triglycerides in milk to provide fatty acids as precursors in the formation of deep eutectic solvent for extraction of polycyclic aromatic hydrocarbons. Talanta. 2022;237:122968.
4. Xu K, Xu P, Wang Y. Aqueous biphasic systems formed by hydrophilic and hydrophobic deep eutectic solvents for the partitioning of dyes. Talanta. 2020;213:120839.
5. Hang NT, Uyen TTT, Phuong NV. Green extraction of apigenin and luteolin from celery seed using deep eutectic solvent. J Pharmaceut Biomed. 2021;207:114406.
6. Xu W, Wang Y, Wei X, Chen J, Xu P, Ni R, Meng J, Zhou Y. Fabrication of magnetic polymers based on deep eutectic solvent for separation of bovine hemoglobin via molecular imprinting technology. Anal Chim Acta. 2019;1048:1–11.
7. Xu K, Wang Y, Huang Y, Li N, Wen Q. A green deep eutectic solvent-based aqueous two-phase system for protein extracting. Anal Chim Acta. 2015;864:9–20.
8. Li N, Wang Y, Xu K, Wen Q, Ding X, Zhang H, Yang Q. High-performance of deep eutectic solvent based aqueous bi-phasic systems for the extraction of DNA. RSC Adv. 2016;6:84406.
9. Zhang H, Wang Y, Zhou Y, Xu K, Li N, Wen Q, Yang Q. Aqueous biphasic systems containing PEG-based deep eutectic solvents for high-performance partitioning of RNA. Talanta. 2017;170:266–74.
10. Nian B, Li X. Can deep eutectic solvents be the best alternatives to ionic liquids and organic solvents: a perspective in enzyme catalytic reactions. Int J Biol Macromol. 2022;217:255–69.
11. Xu P, Wang Y, Chen J, Wei X, Xu W, Ni R, Meng J, Zhou Y. A novel aqueous biphasic system formed by deep eutectic solvent and ionicliquid for DNA partitioning. Talanta. 2018;189:467–79.
12. Chen Y, Liu Y, Shi Y, Ping J, Wu J, Chen H. Magnetic particles for integrated nucleic acid purification, amplification and detection without pipetting. Trac-Trend Anal Chem. 2020;127:115912.
13. Emaus MN, Varona M, Eitzmann DR, Hsieh S, Zeger VR, Anderson JI. Nucleic acid extraction: Fundamentals of sample preparationmethodologies, current advancements, and future endeavors. Trac-Trend Anal Chem. 2020;130:115985.
14. Chen J, Wang Y, Wei X, Ni R, Meng J, Xu F, Liu Z. A composite prepared from MnO_2 nanosheets and a deep eutectic solvent as an oxidase mimic for the colorimetric determination of DNA. Microchim Acta. 2020;187:7.
15. Mondal D, Sharma M, Mukesh C, Gupta V, Prasad K. Improved solubility of DNA in recyclable and reusable bio-based deep eutectic solvents with long-term structural and chemical stability. Chem Commun. 2013;49:9606–8.

16. Sharma G, Sequeira RA, Pereira MM, Maity TK, Chudasama NA, Prasad K. Are ionic liquids and deep eutectic solvents the same?: fundamental investigation from DNA dissolution point of view. J Mol Liq. 2021;328:115386.

17. Xu K, Wang Y, Zhang H, Yang Q, Wei X, Xu P, Zhou Y. Solid-phase extraction of DNA by using a composite preparedfrom multiwalled carbon nanotubes, chitosan, Fe_3O_4 and a poly(ethylene glycol)-based deep eutectic solvent. Microchim Acta. 2017;184:4133–40.

18. Meng J, Wang Y, Zhou Y, Chen J, Wei X, Ni R, Liu Z, Xu F. A composite consisting of a deep eutectic solvent and dispersedmagnetic metal-organic framework (type UiO-66-NH_2) for solid-phase extraction of RNA. Microchim Acta. 2020;187:58.

19. Wang X, Liu M, Peng F, Ding X. Hydrophobic magnetic deep eutectic solvent: synthesis, properties, and application in DNA separation. J Chromatogr A. 2021;1659:462626.

20. Ge J, Xing K, Geng X, Hu Y, Shen X, Zhang L, Li Z. Human serum albumin templated MnO_2 nanosheets are oxidase mimics for colorimetric determination of hydrogen peroxide and for enzymatic determination of glucose. Microchim Acta. 2018;185:559.

21. Sheng E, Lu Y, Tan Y, Xiao Y, Li Z, Dai Z. Oxidase-mimicking activity of ultrath in MnO_2 nanosheets in a colorimetric assay of chlorothalonil in food samples. Food Chem. 2020;331:127090.

22. He L, Lu Y, Wang F, Jing W, Chen Y, Liu Y. Colorimetric sensing of silver ions based on glutathione-mediated MnO_2 nanosheets. Sens Actuator B. 2018;254:468–74.

23. Mu X, Liu X, Ye X, Zhang W, Li L, Ma P, Song D. Branched poly(ethylenimine) carbon dots-MnO_2 nanosheets based fluorescent sensory system for sensing of malachite green in fish samples. Food Chem. 2022;394:133517.

24. Zhang Y, Ma C, Ma C, Xiang Y, Mu S, Zheng Z, Liu X, Zhang H. Ratiometric fluorescent detection and imaging of microRNA in living cells with manganese dioxide nanosheet-active DNAzyme. Talanta. 2021;233:122518.

25. Lyu M, Zhu D, Kong X, Yang Y, Ding S, Zhou Y, Quan H, Duo Y, Bao Z. Glutathione-depleting nanoenzyme and glucose oxidase combination for hypoxia modulation and radiotherapy enhancement. Adv Healthc Mater. 2020;9:1901819.

26. Zhang T, Gan Z, Zhen S, Hu Y, Hu X. Monitoring of glutathione using ratiometric fluorescent sensor based on MnO2 nanosheets simultaneously tuning the fluorescence of rhodamine 6G and thiamine hydrochloride. Spectrochim Acta A. 2022;271:120942.

27. Fan Z, Zhou Z, Zhang W, Zhang X, Lin J. Inkjet printing based ultra-small MnO_2 nanosheets synthesis for glutathione sensing. Talanta. 2021;225:121989.

28. Wang S, Zheng H, Zhou L, Cheng F, Liu Z, Zhang H, Wang L, Zhang Q. Nanoenzyme-reinforced injectable hydrogel for healing diabetic wounds infected with multidrug resistant bacteria. Nano Lett. 2020;20:5149–58.

28. Song H, Wang Y, Wang G, Wei H, Luo S. Ultrathin two-dimensional MnO_2 nanosheet as a stable coreactant of 3,3′,5,5′-tetramethylbenzidine chromogenic substrate for visual and colorimetric detection of iron (II) ion. Microchim Acta. 2017;184:3399–404.

30. Ma K, Liang L, Zhou X, Tan W, Hu O, Chen Z. A redox-induced dual-mode colorimetric and fluorometric method based on N-CDs and MnO_2 for determination of isoniazid in tablets and plasma samples. Spectrochim Acta A. 2021;247:119097.

31. Tian Y, Li Y, Mei J, Deng B, Xiao Y. Hexafluoroisopropanol-modified cetyltrimethylammonium bromide/sodium dodecyl sulfate vesicles as a pseudostationary phase in electrokinetic chromatography. J Chromatogr A. 2015;1404:131–40.

32. Deng W, Zong Y, Xiao Y. Hexafluoroisopropanol-based deep eutectic solvent/salt aqueous two-phase systems for extraction of anthraquinones from rhei radix et rhizoma samples. ACS Sustain Chem Eng. 2017;5:4267–75.

33. Deng W, Yu L, Li X, Chen J, Wang X, Deng Z, Xiao Y. Hexafluoroisopropanol-based hydrophobic deep eutectic solvents fordispersive liquid-liquid microextraction of pyrethroids in tea beverages andfruit juices. Food Chem. 2019;274:891–9.

34. Wang L, Dai D, Chen Q, He M. Rapid and green synthesis of phenols catalyzed by a deep eutectic mixture based on fluorinated alcohol in water. J Fluor Chem. 2014;158:44–7.

35. Zuo Q, Chen Y, Chen Z, Yu R. A novel ratiometric fluorescent sensing method based on MnO_2 nanosheet for sensitive detection of alkaline phosphatase in serum. Talanta. 2020;209:120528.

36. Wang H, Li Y, Bai H, Liu Y. DNA-templated au nanoclusters and MnO_2 sheets: a label-free and universal fluorescence biosensing platform. Sens Actuator B. 2018;259:204–10.

Publisher's Note